

MEASUREMENT AND MODELING ERROR INFLUENCE TO ANTENNA ARRAY CALIBRATION AND ITS AFFECT TO ESPRIT-BASED DOA-ESTIMATION

Gerd Sommerkorn, Dirk Hampicke, Andreas Richter, Reiner Thomä

FG EMT, Ilmenau Technical University
P.O.Box 100565, D-98684 Ilmenau, Germany
Phone: +49 3677 69 1157, Fax: +49 3677 69 1113
Email: { som | ham | ric | tho } @e-technik.tu-ilmenau.de
WWW: <http://www-emt.tu-ilmenau.de>

Abstract – The achievable superresolution performance of DoA-estimation procedures is severely degraded by imperfect antenna array behavior. To tackle against that, array calibration is required. A promising procedure has been described, which is especially well suited as a pre-processing step for ESPRIT-type algorithms. The quality of calibration, however, is affected by various measurement and modeling errors. In this paper, a simulation study on the most important errors is given which includes wavefield distortions caused by non-planar wavefronts, parasitic reflections of the calibration measurement environment, and nonzero relative bandwidth. The resulting performance is demonstrated by unitary ESPRIT-based DoA-estimation. Procedures for enhancement of the quality of calibration are discussed. Measurement results are given, which are based on a wideband vector radio channel sounder¹.

INTRODUCTION

Smart antenna principles are considered to be more and more important for mobile radio. However, adequate performance of antenna arrays requires precise calibration since limited manufacturing accuracy and mutual electromagnetic coupling degrade their performance. Whereas for some array algorithms a precise knowledge of the distorted array steering vector is sufficient, ESPRIT inherently relies on identical beam patterns. In this case, calibration consists in estimation of a calibration matrix, which, in prior to direction of arrival (DoA) estimation, is applied to the received data in order to equalize the distorted beam patterns. A least-square-based algorithm for estimation of the calibration matrix has been described in [1] and its application for vector radio channel measurement has been outlined in [2]. Vector radio channel measurement is carried out in order to precisely analyze the directional radio-wave propagation in a time-variant environment [3]. In this context, the delay-azimuth spectrum is estimated using 2D unitary ESPRIT. The challenging requirements are a dynamic range of better than 35 dB, a rms azimuth DoA error of lower than 0.1 deg., and the ability to resolve closely spaced coherent multipath components. Fortunately enough, the vector radio channel sounder used here contains only a single RF down-converter channel since it is based on fast antenna switching. Therefore, the calibration result can be considered as time-invariant and the calibration measurement can be performed within a special calibration environment. Even though, the result of the calibration is affected by some remaining measurement and modeling errors.

In this paper, the calibration measurement procedure for an uniform linear array (ULA) is shortly outlined, the influences of measurement and modeling errors are analyzed, and procedures for enhancing the quality of calibration are discussed. The calibration results are evaluated by DoA-estimations based on reference data using the unitary 1D-ESPRIT [4]. Finally the simulation results are compared to measurement results.

CALIBRATION PROCEDURE AND SOURCES OF ERRORS

Calibration measurement procedure

The calibration measurement procedure is performed in a well-defined anechoic environment. The reference antenna (Tx) is placed on a grid of N known azimuth angles θ_v , with $v=1(1)N$ within the array azimuth sector of interest. Zero degree azimuth angle stands for the broadside direction. In practice, the reference antenna is kept fixed while the receiver array (Rx array) is being rotated in its axis of symmetry. A minimum distance between Tx antenna and antenna array of approximately 80λ (λ - wavelength) is chosen in order to get nearly plane wavefronts at the antenna array. The desired calibration matrix is determined from the set of the N measured antenna array response vectors by use of an appropriate algorithm [1]. Recently, we demonstrated the calibration of an ULA based on the procedure described above, employing the RUSK ATM vector channel sounder [2] which is based on broadband pseudorandom signal and correlation processing.

¹ This work is supported by the German Federal Ministry of Education, Science and Technology under the ATMmobil project line and the Deutsche Forschungsgemeinschaft. The authors are grateful for cooperation with MEDAV GmbH providing the RUSK ATM vector channel sounder.

Sources of measurement and modeling errors

In practice, however, some of the assumptions of the described calibration measurement procedure cannot be fulfilled truly, leading more or less to impairments of the calibration quality. Major sources of errors might be a non-ideal calibration environment (i.e. if reflectors/echoes are present) and an imperfect mechanical calibration setup (e.g. if the Rx array is not exactly rotated in its radiation center). Moreover, improper distances between Rx array and Tx antenna could be critical since a) the algorithm presumes plane wavefronts which requires very large Rx-Tx separation and b) Rx-Tx distance should be adjusted to a delay bin since that maximizes the impulse response amplitude. In order to investigate the different error sources separately, computer simulations are necessary. In the following section simulation results are discussed, which consider the sources of error separately as well as jointly. The calibration results are evaluated by means of an ESPRIT-based DoA-estimation. In addition, these results are compared with data from real calibration measurements.

SIMULATION AND MEASUREMENT RESULTS

Simulation scheme

The simulation setup has been chosen according to a realistic measurement setup in a typical anechoic chamber (Fig. 1). Generally, the simulation considers two different types of data sets. The first one results from plane wavefronts. The second one is based on a geometrically realistic scenario and therefore spherical wavefronts are considered. Both sets are simulated a) for the ideal echo-free case and b) under the influence of one parasitic echo which may result from a fixed plane reflector in the environment. The frequency domain array output vector are generated for an eight element ULA for different Tx positions within the Rx array 3dB beamwidth. Those data sets were modified by a unique (frequency invariant) error matrix which represents the mutual coupling effects within the antenna array. Frequency-variant coupling was considered in [2]. The error matrix was derived from a field simulation program and can be characterized as the inverse calibration result of an eight element ULA. In order to estimate the proper calibration matrix for each data set, only the strongest delay bin is used which is related to the Tx antenna reference. For that aim, the impulse response is calculated from the frequency response vector via the inverse Fourier-transform. The impulse response envelope of any single delayed path will be sinc-shaped since a rectangular windowing function was used in the frequency domain. Now, the calibration matrix for each data set is estimated using the algorithm in [1]. Afterwards, the calibration matrix is applied to a reference data set that can be considered as an error-free calibration measurement set influenced only by the error matrix. Finally, the unitary 1D-ESPRIT is employed in order to determine the resulting DoAs. Since the desired calibration scenario is supposed to consist of one path, the model order deliberately was fixed to 1. In order to evaluate how this idealized model assumption is disturbed by the different sources of errors, an appropriate model error is introduced. This model error is defined by the deviation (in dB) of the measured reference delay bin (which contains no modeling assumption) from the resynthesized one (based on the ESPRIT based model parameter estimate).

simulation parameter	values
distance between Tx antenna and Rx array (pivot)	2.5 m ... 500 m (default: 5 m)
Tx antenna path weight	magnitude: 0 dB; phase: 0°
relative bandwidth (assumed carrier frequency @ 5.2 GHz)	0.1 % ... 5 % (default: 2.3 %)
mismatch between the array axis of symmetry and the pivot	$x,y \in \{-0.25\lambda, 0, 0.25\lambda\}$ (default: $x,y = 0\lambda$)
array interelement spacing	0.4λ
array orientation θ_r (broadside of the array, related to the Tx angle of incidence = 0°)	-60° (3°) +60°
reflection angle of incidence regarding broadside of the array	-30° (5°) 0°
additional const. path distance due to reflection (along an ellipse)	3.75 m
reflection path weight	magnitude: -30 dB (10 dB) -10 dB; phase: 0° (45°) 315°

Table 1 Major parameter used for the simulation

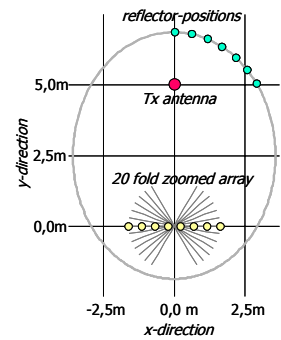


Fig. 1 Simulation setup

Table 1 shows the major parameters and the respective ranges of values which were used for the simulation. The first part of the simulation considers variations of the Tx-Rx distance, of the relative bandwidth, and the mismatch of the array rotation axis. For the latter case a second point is introduced – denoted as pivot – which describes the deviation of the rotation axis from the Rx array axis of symmetry. The second part of the simulations focuses on the influence of a parasitic echo. The echo is simulated with time-delay relative to the Tx path which equals the first side lobe of the rectangular window function in the respective impulse response. For simplification, free space path loss has been neglected for all simulations and moreover, only integer multiples of the delay resolution were used for the Tx- pivot distance.

Simulation results excluding reflections

The influence of spherical wavefronts on the DoA-estimation vs. the Tx-Rx distance is depicted in Fig. 2. Both, the relative bandwidth (2.3%) and the pivot were set to their default values. It can be seen clearly, that errors are reduced significantly for larger distances, since the wavefronts become more and more plane and therefore a better match to the calibration model is given.

The error characteristics in Fig. 3 demonstrate the influence of spherical wavefronts vs. the relative bandwidth for a fixed distance of 5m. It can be seen that the variation of the two different parameters in Fig. 2 and Fig. 3 leads to the same behavior. In case of plane wavefronts, this parameters have no influence.

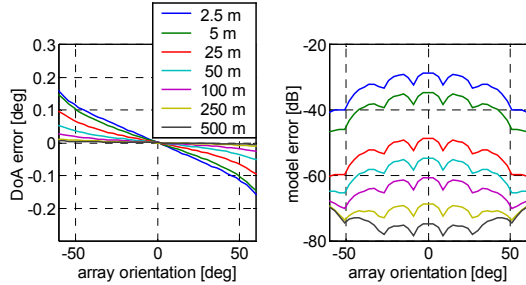


Fig. 2 Error characteristics for spherical wavefronts dependent on the Tx-Rx distance

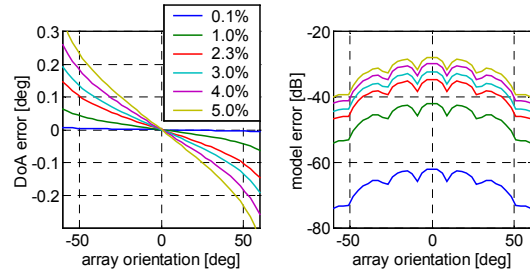


Fig. 3 Error characteristics for spherical wavefronts dependent on the relative bandwidth

Fig. 4 shows the simulation results in case of a pivot offset which exists in x- as well as in y-direction. While plane wavefronts have obviously no influence, for spherical wavefronts the results are impaired.

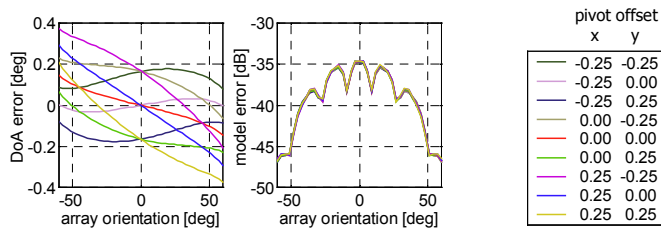


Fig. 4 Error characteristics for spherical wavefronts dependent on the pivot offset (x-offset and y-offset in λ)

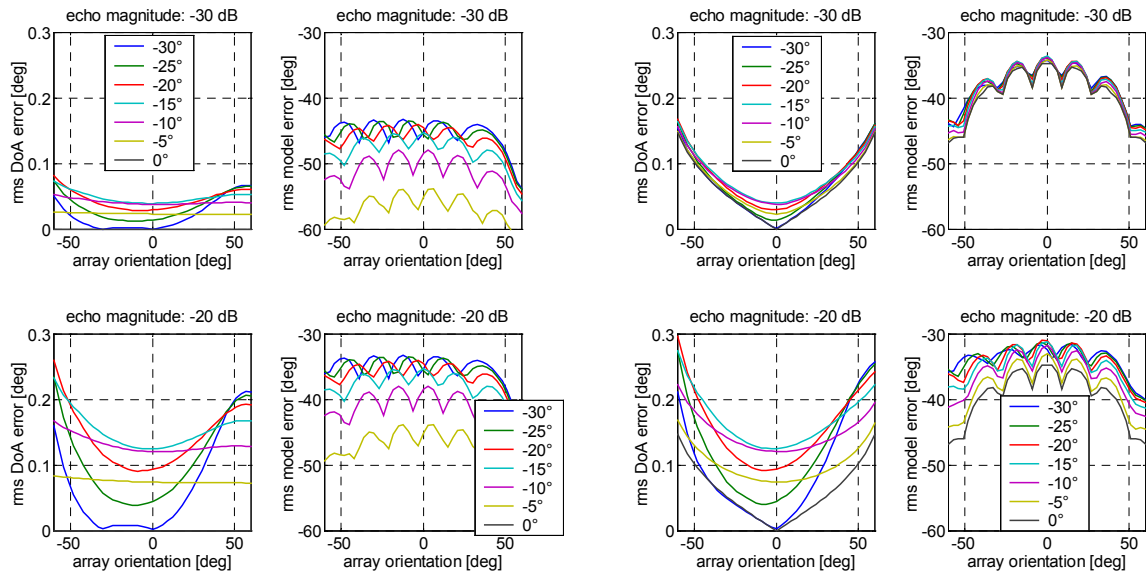


Fig. 5 Echo influence on plane wavefronts (upper: -30 dB; lower: -20 dB echo magnitude)

Fig. 6 Echo influence on spherical wavefronts (upper: -30 dB; lower: -20 dB echo magnitude)

Simulation results including reflections

If parasitic echoes exceed a certain amplitude, this will lead to obvious deformations of the wave pattern for the calibration single-source scenario. Depending on the location and the phase of the echo, the deformations will be quite different. Therefore in the simulation, the complex valued echo path weight and the angle of incidence of the echo were modified. Generally, the simulation results were rms averaged over 2π variation of the echo phase.

In Fig. 5 and Fig. 6 the influence of an echo which impinges during the calibration measurement is depicted. For reasons of symmetry only, the range between $-30^\circ(5^\circ)0^\circ$ is considered. It is remarkable that for smaller echoes (approx. -30dB) the influence of spherical wavefronts is more dominant, while for stronger echoes (approx. -20dB) this effect can be more and more neglected, i.e. the behavior of the simulation is equal for plane and spherical wavefronts.

Measurement results

Fig. 7 shows the result of the calibration of the RUSK ATM antenna array. The pre-processing of the measurement data and the application of the calibration algorithm were chosen equivalent to the simulation, as described before. However, the results have to be considered as somewhat idealized. Since there was no independent reference available, the evaluation of the calibration results is based on the same measured data sets which was also used for the calibration itself. Even though, the measurement example shows what can be achieved in practice.

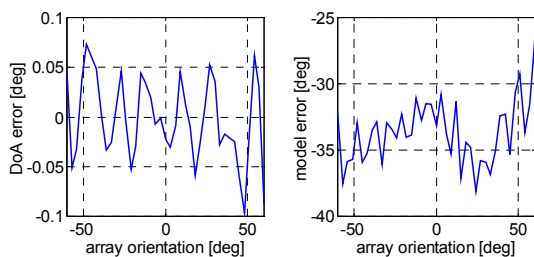


Fig. 7 Calibration measurement results

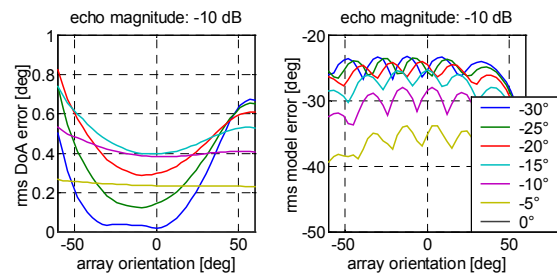


Fig. 8 Influence of strong echoes on plane wavefronts

CONCLUSIONS

In this paper, we have shown the influences of different error sources on the calibration of antenna arrays by means of simulations. We also verified the results by measurements. It turns out that echoes may have a large impact on the calibration quality. Also, spherical wavefronts have a disturbing effect. Further work is devoted to find methods to reduce these influences. Parasitic echoes should be kept as low as possible by using an anechoic environment. A highly directive Tx antenna can also contribute to echo reduction. If all that means cannot be applied (or are not enough), an ESPRIT-based joint estimation procedure of the direct path and the delayed components is proposed, in order to remove the echo contributions. First simulation results have shown that even a very strong echoes, e.g. as given by (Fig. 8), can be completely removed in case of plane wavefronts. But there is a strong influence of spherically shaped waveforms and of other errors. Therefore, detailed investigations to verify this by simulation which takes into account multiple error contributions and by means of measurements are still in progress.

REFERENCES

- [1] K.Pensel, J.A. Nosseck, "Uplink and Downlink Calibration of an Antenna Array in a Mobile Communication System", *COST 259, 3rd Meeting*, TD-58, Lisbon, Portugal, Sept. 1997.
- [2] G. Sommerkorn, D. Hampicke, R. Klukas, A. Richter, A. Schneider, R. Thomä, "Reduction of DoA Estimation Errors Caused by Antenna Array Imperfections", *Proc. 29th European Microwave Conference*, Munich, vol. 2, pp. 287-290, Oct. 4-8, 1999
- [3] R.S. Thomä, D. Hampicke, A. Richter, G. Sommerkorn, A. Schneider, U. Trautwein, W. Wirnitzer, "Identification of Time-Variant Directional Mobile Radio Channels", to appear in: *IMTC/99 Special Issue of IEEE Trans. on Instrumentation and Measurement*, April 2000
- [4] M.Haardt, J.A.Nosseck, "Unitary ESPRIT: How to Obtain Increased Estimation Accuracy with a Reduced Computational Burdon", *IEEE Transactions on Signal Processing*, vol. 43, no. 5, pp. 1232-1242, May 1995.